Received: 14 November 2022 | Revised: 28 January 2023 | Accepted: 1 February 2023

DOI: 10.1002/app.53760

RESEARCH ARTICLE

Journal of Applied Polymer Science WILEY

Photo-oxidation of poly(diethylene glycol terephthalate)

Fiona J. Horne | **John J. Liggat**

Department of Pure and Applied Chemistry, University of Strathclyde, Glasgow, Scotland

Correspondence
John J. Liggat, Department of Pure and Applied Chemistry, University of Strathclyde, Glasgow, G1 1XL, Scotland, UK.
Email: j.j.liggat@strath.ac.uk

Abstract

The photo-oxidation of poly(diethylene glycol terephthalate) (PDEGT) under accelerated aging conditions has been investigated. A weatherometer was used to expose samples to simulated sunlight under air, replicating outdoor exposure. Irradiations were also performed under air using UV lamps of wavelengths centred on 302 and 365 nm. After exposure, the extent of degradation was determined using attenuated total reflectance Fourier transform infrared spectroscopy, diffuse reflectance infrared Fourier transform spectroscopy and UV–visible spectroscopy. Results show that in general PDEGT degrades to a greater extent than the closely-related polymer poly(ethylene terephthalate) due to the susceptibility of the ether linkage. Although the diethylene glycol sequences are not themselves photoactive over this wavelength range and are not acting as photochemical weak links they do serve as additional sites for secondary free radical chemistry.

KEYWORDS

FTIR, photodegradation, poly(diethylene terephthalate), UV irradiation, weathering

1 | INTRODUCTION

Diethylene glycol (DEG) is used as a comonomer in the production of poly(ethylene terephthalate) (PET), mainly for its role as a processing aid. DEG ether groups provide some degree of flexibility to a relatively stiff PET backbone, which slows its crystallization. This property is used, for example, to reduce the hazing observed upon cooling of blow-molded objects such as PET bottles. However, DEG sequences can form during through unwanted side reactions during the polymerization of PET.[1–3] DEG units have been known to be weak points in the thermal and thermo-oxidative degradation of PET for quite some time since Pohl originally reported the fact in 1951.[4–12] The major conclusions accumulated over the years were that poly(diethylene glycol terephthalate), PDEGT, degraded at lower temperature and faster than PET, and that DEG units were particularly sensitive to oxidation.

In contrast, the photochemistry of PDEGT and the possible role of DEG as an internal weak link during outdoor weathering of PET has been much less well studied. Indeed, we are not aware of any published work despite the increased use of PET in applications such as backsheets for photovoltaic cells. In a recent paper[13] we described the photodegradation of PET film under artificial weathering conditions. A weatherometer was used to expose samples to a broad wavelength range of light in an oxidative environment, replicating outdoor solar exposure. Irradiations were also performed using UV lamps of wavelengths 302 and 365 nm light, in an oxidative environment. Results showed the production of a series of degradation products, including carboxylic acid end groups, anhydrides, aldehydes, quinones, and monohydroxy terephthalate groups. In this paper we extend that study to the artificial weathering of PDEGT under

conditions replicating outdoor solar exposure and to more specific irradiation at 302 and 365 nm under oxidative conditions. Weathering was undertaken in an Atlas Suntest XLS+ weatherometer, and irradiations were performed using UVP XX-series bench lamps of wavelengths 302 and 365 nm and a Hönle Cube 100 UV lamp of wavelength 365 nm. A photodegradation cell was used to expose samples at different temperatures and atmospheres. After exposure, the extent of degradation was analyzed using ATR FT-IR, DRIFT and UV–Vis–NIR.

2 | MATERIALS AND EXPERIMENTAL

2.1 | Polymer

The PDEGT homopolymer was supplied by DuPont Teijin Films®. PDEGT was precipitated from a 10% w/v solution in chloroform into a bath of isopropanol cooled by liquid nitrogen to the slush point, to remove any oligomers from the material The polymer was then dried under vacuum. Samples for artificial weathering and UV irradiation were prepared by dissolving the purified PDEGT in dichloromethane at ~10% w/v, solvent casting onto aluminium foil and drying under vacuum. FTIR spectra and the mass of the samples were recorded to track the drying process. A digital external micrometer with a range of 0–25 mm was used to measure the thickness of each of the dry films.

2.2 | Weathering and UV irradiation conditions

Weathering experiments were performed in an Atlas Suntest XLS+ weatherometer using a daylight filter with a cut-off at 290 nm (see supplementary material, Figure S1). Exposures were carried out according to ASTM D5071-06 *Exposure of Photodegradable Plastics in a Xenon Arc Apparatus*. A SunCal calibration sensor was used to calibrate the weatherometer before starting a new programme. The sensor allows simultaneous calibration of both irradiance and BST. This weatherometer model follows ISO 4892-1 for measuring and controlling the maximum surface temperature of a black sample. The films were exposed to an irradiation intensity of 365 ± 35 W m^{-2}, measured between 290–800 nm, and a black standard temperature, BST, of 37.5 ± 2.5°C. Samples were irradiated for 6 weeks (equivalent to a dosage of approximately 3.7 x 10^5 W m^{-2} h) and analyzed every week. One week of irradiation in the weatherometer is equivalent to approximately 3.5 weeks outdoor exposure at the UK average.[14]

UV irradiations, under narrower wavelength ranges, were performed using UVP XX-series bench lamps of wavelengths 302 and 365 nm. These produce wavelength bands centred on 302 and 365 nm (see supplementary material, Figure S2) but are referred to as the 302 and 365 nm lamps throughout this paper. Irradiations were mostly carried out at room temperature under air.

Some UV irradiations were also performed using a high intensity Hönle LED Cube 100 lamp of wavelength 365 nm. The LED source is both more intense and of narrower wavelength distribution than the UVP lamps (see supplementary material, Figure S3). The samples were exposed to an average intensity of 825.5 ± 20 W m^{-2} at a temperature of 43 ± 2.5°C. Samples were exposed for 1 week and analyzed every 24 h.

2.3 | Infrared spectroscopy

An Agilent ATR 4500 FT-IR spectrometer was used in the range of 4700–650 cm^{-1}, with a resolution of 2 cm^{-1} and number of scans set to 64. An Agilent Exo-Scan 4100 was used to collect DRIFT spectra in the range of 5200–650 cm^{-1}, with a resolution of 4 cm^{-1} and number of scans set to 128. Four spectra were taken at points across the surface and averaged each time the sample was analyzed. ATR is a surface technique with a penetration depth of approximately 2 to 5 μm whereas DRIFT is a technique which allows the bulk of the sample to be analyzed with a penetration depth of approximately 400 μm. Analysis of the spectra included baseline correction and normalization to the peak at 1410 cm^{-1} that is assigned to aromatic skeletal stretching and considered to be relatively invariant during the weathering process.

2.4 | UV–visible-near IR spectroscopy

UV–visible-NIR spectroscopy was conducted using a UV-1800 UV–visible Spectrophotometer with a scan range of 190–600 nm.

2.5 | Characterization of PDEGT

DSC analysis (supplementary information, Figure S4) of the purified and precipitated PDEGT show it to be semicrystalline with a T_g of 25°C and twin melting peaks, T_{m1} 58°C and T_{m2} 92°C, reflecting two distinct crystalline morphologies. The polymer does not crystallize from the melt upon cooling to room temperature at 10°C min^{-1} or upon reheating. As cast from dichloromethane as films for weathering and UV irradiation, the PDEGT was amorphous with a T_g of 23°C and remained in this state subsequently.

The ATR-IR and DRIFT spectra for purified PDEGT are shown in Figure 1a and b, respectively. The band assignments for the peaks in these spectra are given in Table 1.

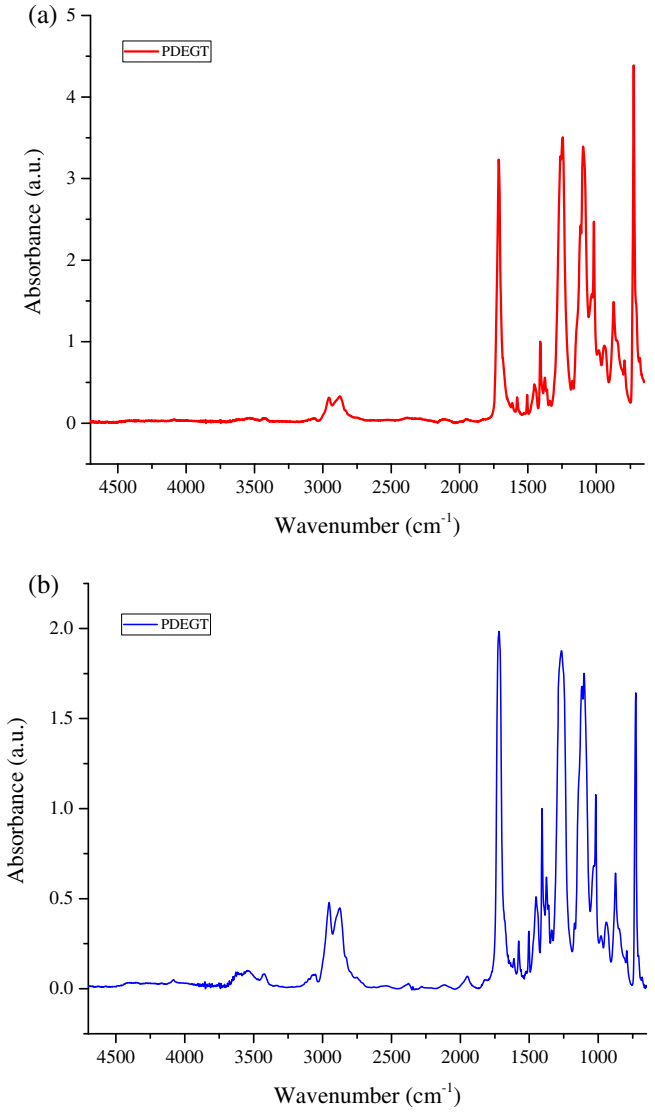

FIGURE 1 (a) ATR FT-IR and (b) DRIFT spectra of purified PDEGT. [Color figure can be viewed at wileyonlinelibrary.com]

The UV–visible spectrum of PDEGT is shown in Figure 2. This shows that short wavelengths, between 280–325 nm, are absorbed strongly, whereas longer wavelengths, between 325–450 nm, are absorbed less. The spectrum is very similar to that of PET, being dominated by the n-π* transition of the ester carbonyl.

3 | RESULTS AND DISCUSSION

3.1 | Weatherometer exposure

3.1.1 | ATR-FTIR

Figure 3 shows the ATR spectra for PDEGT after every week of exposure in the weatherometer. Even after only 1 week of exposure, there are substantial changes in the spectrum in the region between 3800–2100 cm^{-1}, as well as in the carbonyl and fingerprint regions. Peaks are assigned in Table 2.

The region of the spectra between 3800–2100 cm^{-1}, containing the -COOH and -OH peaks as well as the aromatic and aliphatic C-H stretching peaks, for the control and the PDEGT sample weathered for 6 weeks, is shown in Figure 4. The peak at 3290 cm^{-1} has been assigned to free carboxylic acid group and has developed during weathering.[15] Of particular note are the peaks at 2665

TABLE 1 Band assignments for the ATR FT-IR and DRIFT spectra of PDEGT (collated from refs 9, 15, 16)

Wavenumber (cm^{-1})		
ATR FT-IR	DRIFT	Assignment
3630	3620	Moisture
3550	3540	R-O-H stretching vibration
3430	3425	First overtone of the carbonyl peak
3100–3060	3100–3060	Aromatic C-H stretching
2955, 2875	2955, 2875	Aliphatic CH_2 stretching
1950	1950	Aromatic summation band
1720, 1713	1720	Amorphous and crystalline carbonyl stretching
1614, 1453, 1439, 1409	1612, 1451, 1436, 1409	Aromatic skeletal stretching bands
1578, 1505	1577, 1504	Amorphous and crystalline ring stretching
1265	1265	C(O)-O stretching of ester group
1173, 1115, 1017	1173, 1117, 1017	Indicative of aromatic 1, 4-substitution pattern
1095	1104	C-O stretching vibration of aliphatic ester
980	980	O-CH_2 stretching of ethylene glycol segment
940	940	O-CH_2 stretching of diethylene glycol segment
873	874	Isolated hydrogen on aromatic ring
845	845	C-H deformation of two adjacent hydrogens on the terephthalic ring
726	727	Out of plane deformation of the two carbonyl substituents on the aromatic ring

and 2550 cm^{-1}, representative of the carboxylic acid dimer.[17] Carboxylic acid dimers have been reported in the literature by Delprat et al. during the photodegradation of copolymers[18] and the production of carboxylic acid end groups has been reported in the literature for PET materials[15,19,20] and Fechine et al. have proposed a pathway (Scheme 1) for the production of these groups during the photo-oxidation of PET.[21] The mechanism is likely to be the same for the weathering of PDEGT.

The C-H stretching region between 3100–2750 cm^{-1} is difficult to interpret due to the overlap with the strong underlying -OH and -COOH absorbances but it does look

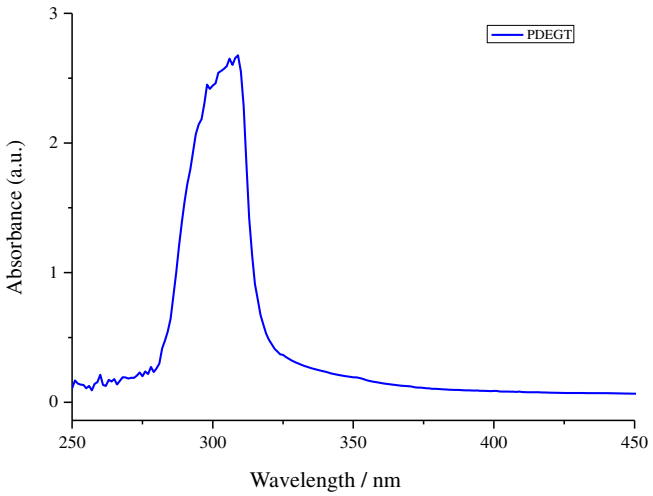

FIGURE 2 UV–visible spectrum of PDEGT between 250–450 nm. [Color figure can be viewed at wileyonlinelibrary.com]

TABLE 2 Band assignments for the region between 3800–2100 cm^{-1} of the ATR FT-IR spectrum of weathered PDEGT (collated from refs. 9, 15–17, 22, 23)

Peak (cm^{-1})	Assignment
3630	Moisture
3550	R-O-H stretching vibration
3430	First overtone of the carbonyl peak
3290	Carboxylic acid end groups
3100–3060	Aromatic C-H stretching
2955, 2875	Asymmetric and symmetric aliphatic C-H stretching
2920	C-H symmetric stretching vibration associated with the Ar-CH_3 group[5]
2665, 2550	Characteristic of the carboxylic acid dimer[6]

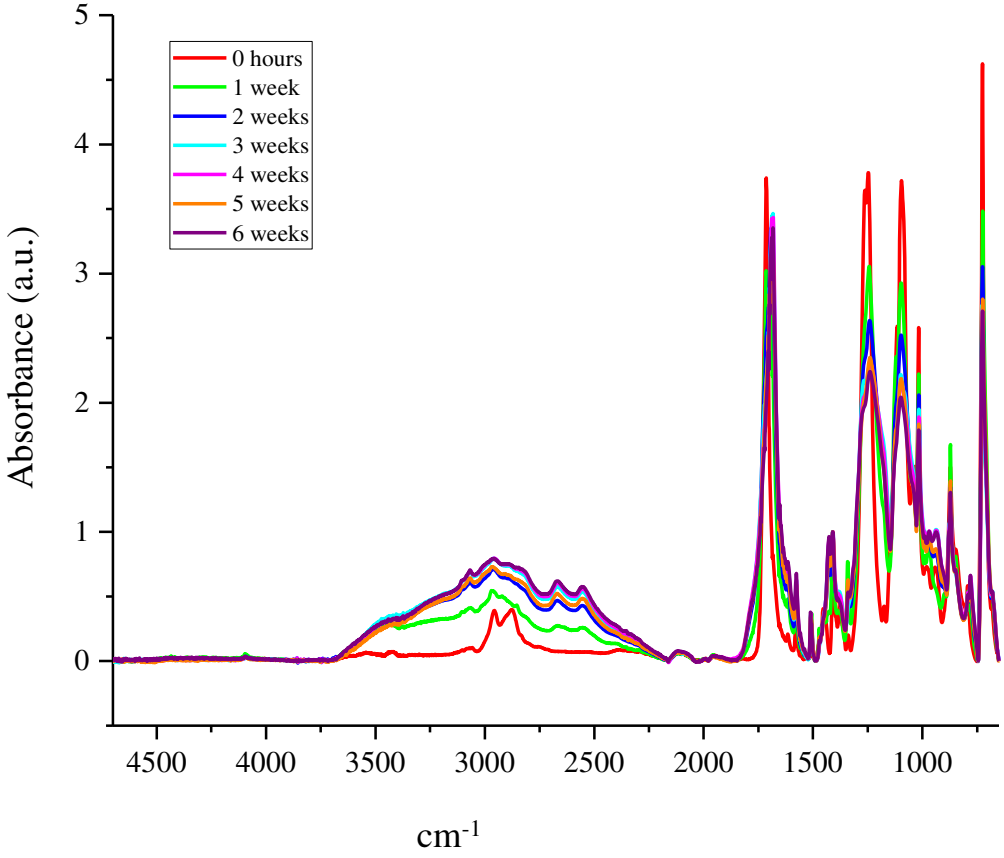

FIGURE 3 ATR FT-IR spectra of PDEGT weathered from 1–6 weeks. [Color figure can be viewed at wileyonlinelibrary.com]

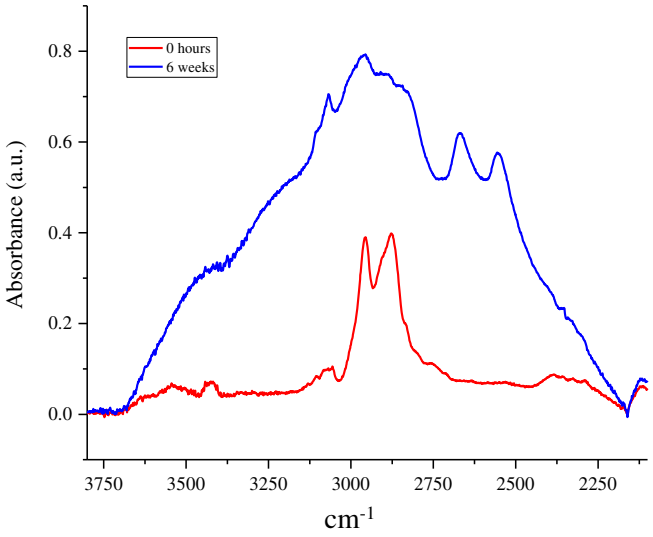

FIGURE 4 ATR FT-IR spectrum in the region between 3800–2100 cm^{-1} of PDEGT weathered for 6 weeks. [Color figure can be viewed at wileyonlinelibrary.com]

as if the aliphatic C-H peak has reduced in intensity relative to the neighboring aromatic C-H. This is consistent with preferential oxidation of the glycol C-H sequences. Upon exposure, another peak has developed at 2920 cm^{-1} and has been assigned to the C-H stretching vibration associated with the Ar-CH_3 group. It is thought that phenyl and methyl radicals could be produced and combine to form an Ar-CH_3 group in a non-oxidative pathway. These radicals have been shown to be produced during the photodegradation of other polyesters.[24]

The change in the carbonyl peak upon weathering for 6 weeks is shown in Figure 5. The peaks contained within the carbonyl peak envelope after exposure are given in Table 3.

Of immediate note is that, upon weathering, the ester carbonyl peak is seen to broaden markedly. This is expected as chain scission reactions can occur at the ester group, as shown in PET [ref 13 and references therein] leading to the production of new carbonyl environments

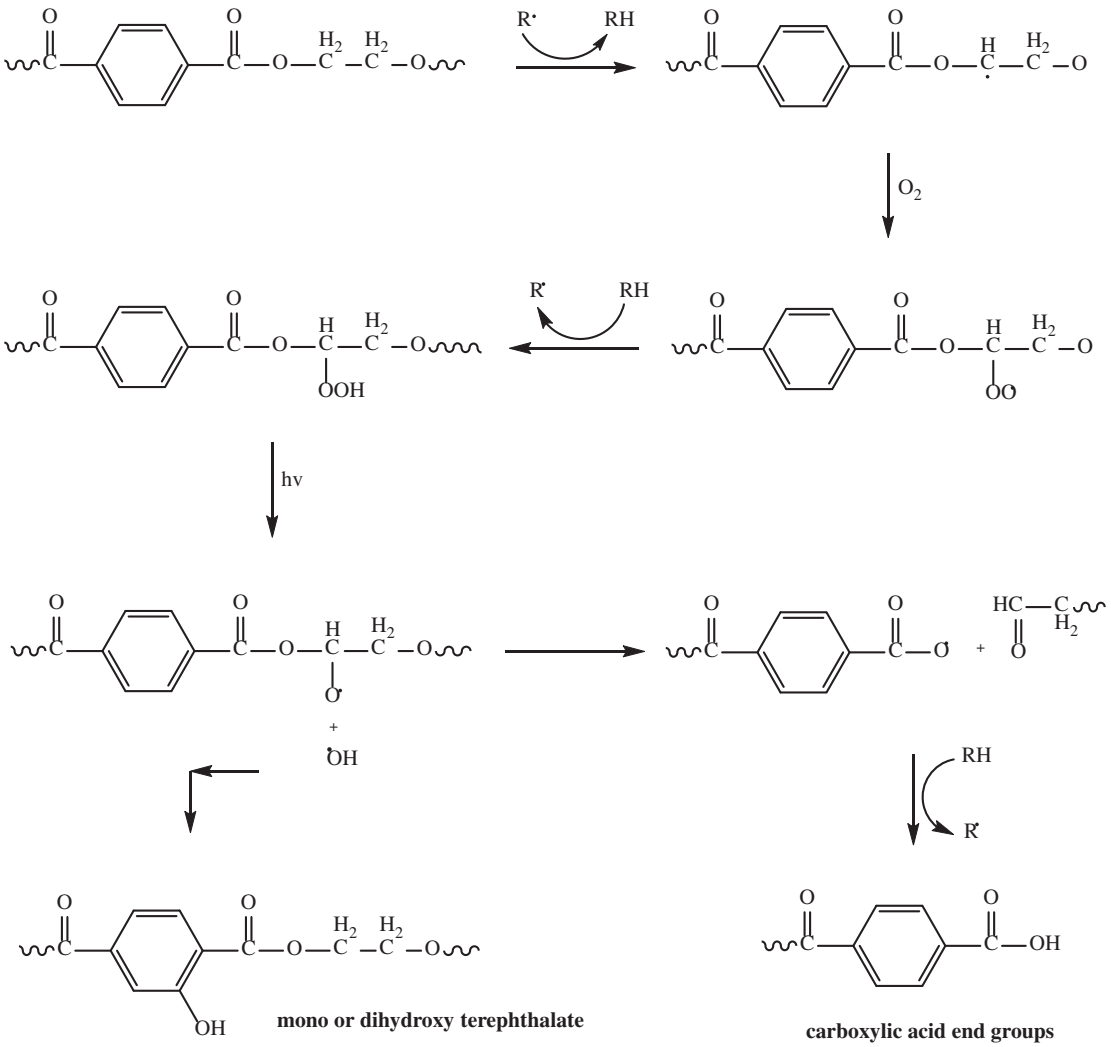

SCHEME 1 Fechine et al. proposed photo-oxidation reactions undergone by PET when exposed to UV light. Radicals R can be produced either by a Norrish Type I reaction or in this reaction cycle.[21]

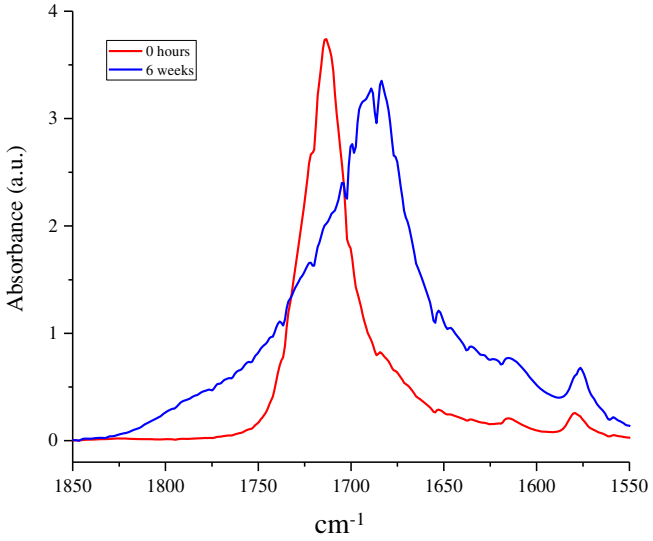

FIGURE 5 ATR FT-IR spectrum in the carbonyl region between 1850–1550 cm^{-1} of PDEGT weathered for 6 weeks. [Color figure can be viewed at wileyonlinelibrary.com]

and a consequent general broadening of the carbonyl peak. For example, the broadening to higher wavenumbers has been assigned to the formation of anhydride groups. The formation of anhydride groups has been reported by Scheirs and Gardette during the photo-oxidation of PEN but not PET[25] although we have subsequently shown that anhydrides do form in the photo-oxidation and weathering of PET.[13] It is very plausible, therefore, that anhydrides could also be produced during the exposure of PDEGT. Aliphatic aldehydes from the oxidation of the glycol sequences would also contribute to this broadening to higher wavenumbers.[19]

The broadening of the carbonyl peak at lower wavenumbers is due to the development of peaks at 1700, 1695, 1690 and 1685 cm^{-1}, attributed to the carboxylic acid dimer, end groups, quinone groups and terephthalic acid. Quinone groups have been identified during the photodegradation of PET by Edge et al., reporting changes in IR spectra and Fechine et al., showing changes in UV–visible spectra.[28,29] Both groups proposed mechanistic pathways have been proposed for their production. The peak at 1685 cm^{-1}, assigned to terephthalic acid, is suggestive of ester scission reactions.[28]

Figure 6 shows the fingerprint region of a control sample and a film weathered for 6 weeks. The various peaks that have changed or developed during exposure have been assigned in Table 1.

The evolution of peaks at 1430 and 1220 cm^{-1} are associated with the production of the carboxylic acid dimers commented upon earlier. Peaks at 1265 and 1095 cm^{-1}, associated with the ester group show a decrease in absorbance with exposure time. This again indicates that ester scission reactions have occurred during exposure. Figure 6 also shows the reduction in size of the peaks at 980 and 940 cm^{-1}, assigned to the O-CH_2 stretching of the ethylene glycol and diethylene glycol segments, respectively.[9] The reduction in size of these peaks indicates the breakdown of the ether units during degradation.

TABLE 3 Band assignments for the carbonyl region of the ATR FT-IR spectrum of PDEGT (collated from refs 18,22,23,25-27)

Peak (cm^{-1})	Assignment
1785	Carbonyl stretch from anhydride carbonyl
1740	Carbonyl stretch from aliphatic aldehyde
1720	Carbonyl stretch from backbone ester
1700	Carbonyl stretch from carboxylic acid dimer
1695	Carbonyl stretch from carboxylic acid end groups
1690	Carbonyl stretch from quinone groups
1685	Carbonyl stretch from terephthalic acid

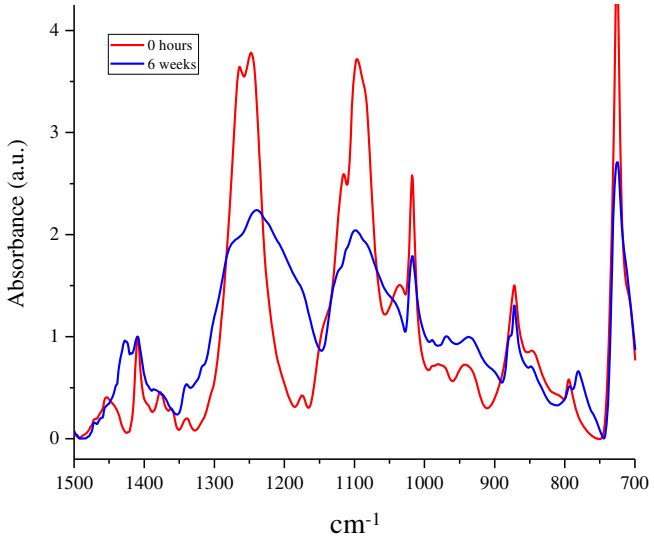

FIGURE 6 ATR FT-IR spectrum in the fingerprint region between 1500–700 cm^{-1} of PDEGT weathered for 6 weeks. [Color figure can be viewed at wileyonlinelibrary.com]

TABLE 4 Band assignments for the UV–Vis–NIR spectra of PDEGT

Wavelength (nm)	Assignment
2265, 2450	Combination C-H stretching
1925	Combination O-H stretching
1715, 1660	First overtone C-H stretching
845	Third overtone C-H stretching

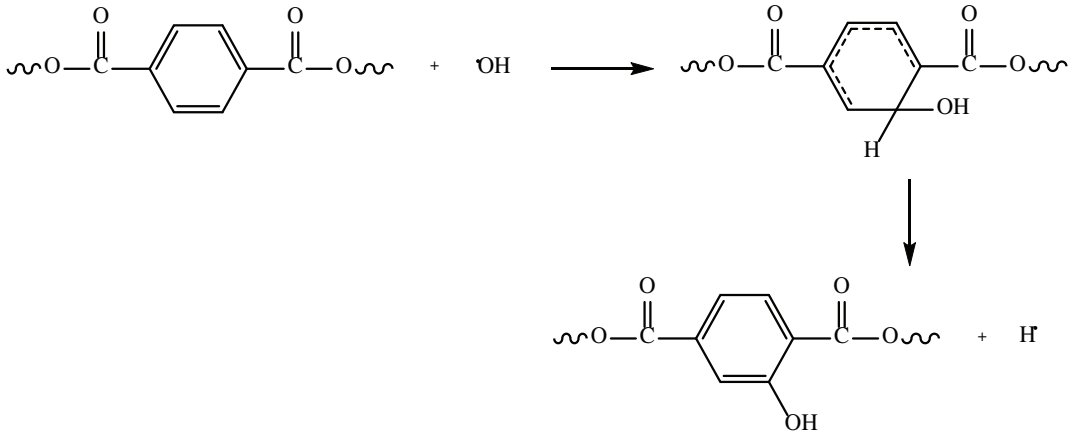

SCHEME 2 Mechanism for the formation of monohydroxy terephthalate groups in the polymer backbone, including hydroperoxide formation and photolysis as proposed by Day and Wiles.[31]

The region between 850–750 cm^{-1} is sensitive to changes in the substitution pattern of the terephthalic ring. After exposure, there has been change in the peak at 845 cm^{-1} and development of peaks at 778 and 758 cm^{-1}. From Figure 6, it is apparent that there has been a small reduction in the size of the peak at 845 cm^{-1} assigned to the C-H deformation of two adjacent hydrogens on the terephthalic ring. This suggests that substitution has occurred on the ring.[9,16] This is further supported by the development of the peaks at 758 cm^{-1} assigned to the 1,2,4 tri-substituted ring.[23] The change and evolution of these peaks support the formation of monohydroxy terephthalate groups. The monohydroxy terephthalate groups were first identified by Pacifici and Straley[30] and a mechanism (Scheme 2) was proposed for their formation by Day and Wiles.[31]

The development of the peak at 778 cm^{-1} upon weathering has only been reported once for PET[13] and is thought to be due to mono-substituted rings. The peak that has developed here is more pronounced compared to the evolution of the peak during weathering of PET.[13] For PET, we proposed that the structure arose from a phenyl radical abstracting a hydrogen atom from the backbone of the polymer chain. In PDEGT there are more hydrogen atoms available in the main chain, due to the incorporation of the diethylene glycol segment. This means that it will be easier for the phenyl radical to abstract a hydrogen and thus more mono-substituted rings will be produced.

It is important to compare the degradation of the PDEGT with PET under the same conditions. An estimate of the overall extent of photodegradation of PDEGT was obtained in the same way as for PET[13] viz monitoring the change in area with dosage of the regions between 3800–2100 cm^{-1} and the 1880–1550 cm^{-1}. Figure 7 shows the change in area of these regions. Data for PET[13] is included for reference. Both graphs show an initial sharp increase in area, followed by a more moderate increase for PDEGT. In comparison to PDEGT, PET shows only minor increases with dosage. Thus under similar weathering conditions PDEGT degrades to a much greater extent than PET. This immediately suggests that the ether linkage is the weak link in PDEGT, as for thermal degradation, as this is the only structural difference between the two polymers.

3.1.2 | Drift

DRIFT spectra differ somewhat from ATR-FTIR spectra as DRIFT analyses the whole thickness of the film, whereas ATR-FTIR only analyses the surface of the film. In addition, due to differential depth penetration of the evanescent wave at the crystal-sample interface, ATR-FTIR spectra give greater prominence to peaks at low cm^{-1} relative to DRIFT. Peak assignments are the same as for ATR-FTIR.

Figure 8 shows the full DRIFT spectra for a control sample and PDEGT irradiated in the weatherometer for up to 6 weeks. Figures 9 - 11 show localized regions of the DRIFT spectra for samples aged for 6 weeks. Trends are very much the same as those determined by ATR-FTIR suggesting that weathering has occurred throughout the depth of the sample and has not been confined to the surface.

Using the DRIFT spectra, the extent of photodegradation of PDEGT was measured in the same way as by ATR. Figure 12a and b show very similar trends to the ATR data.

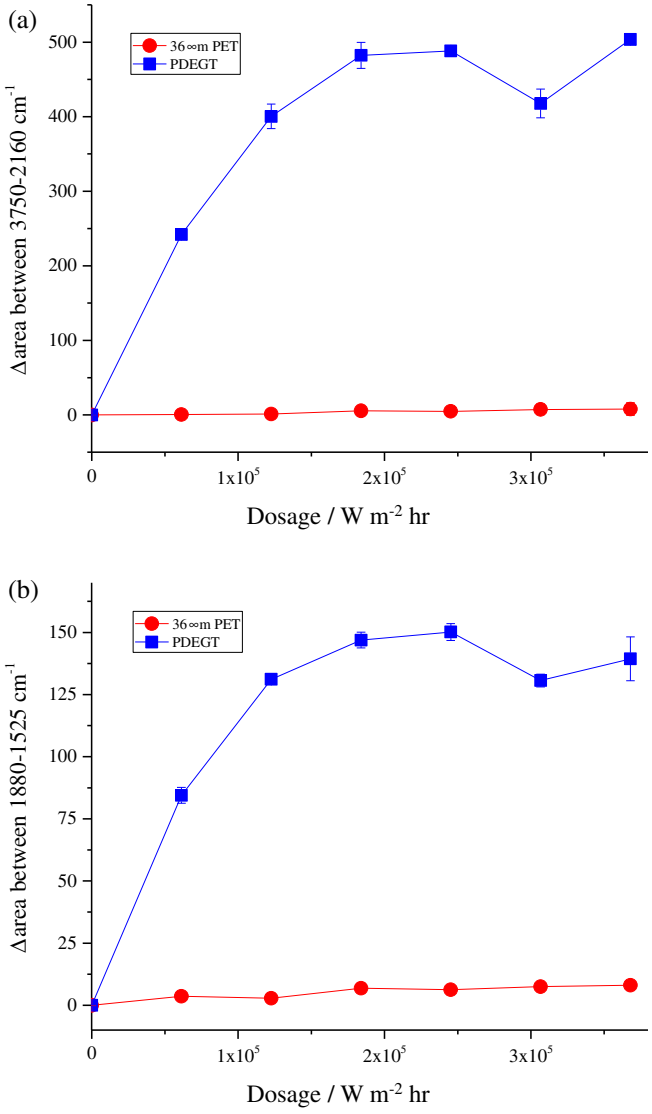

FIGURE 7 Extent of photodegradation of PDEGT measured by the change in area of peaks between (a) 3750–2160 cm^{-1} and (b) 1880–1525 cm^{-1}(carbonyl). Data for PET from ref 13 is included for comparison. [Color figure can be viewed at wileyonlinelibrary.com]

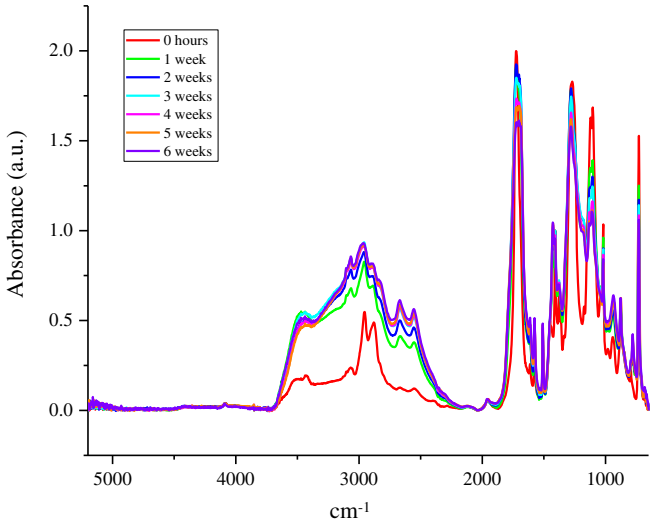

FIGURE 8 DRIFT spectra of PDEGT films irradiated in the weatherometer for 6 weeks. [Color figure can be viewed at wileyonlinelibrary.com]

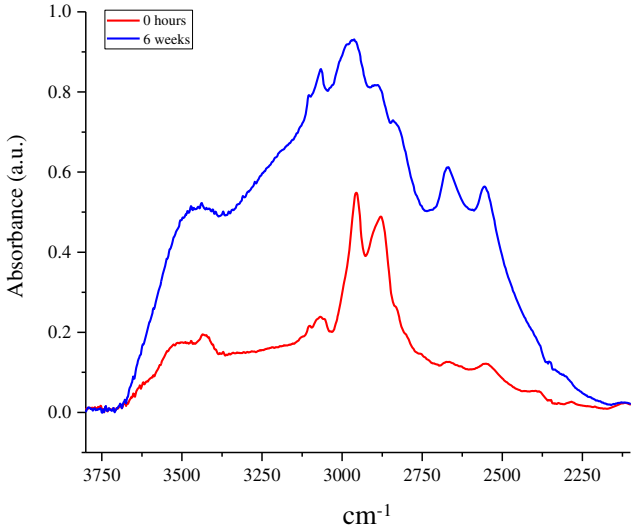

FIGURE 9 DRIFT spectra of PDEGT irradiated in the weatherometer, in the region between 3800–2100 cm^{-1}. [Color figure can be viewed at wileyonlinelibrary.com]

3.1.3 | UV–Vis–NIR

Figure 13 shows the UV–Vis–NIR spectra of samples irradiated in the weatherometer for 24 h and 1 week. The peaks in the spectra have been assigned in Table 4. Peaks at 2265 and 2450 nm have been assigned to a combination C-H stretching, while 1715, 1660 and 845 nm have been assigned to the first overtone and third overtone of the C-H stretching.

After 1 week of weathering it is apparent that there has been a development of a peak at 1925 nm which has been assigned to the combination O-H stretching peak. This indicates the production of new hydroxy groups during the photodegradation of PDEGT, which could include carboxylic acid end groups. After weathering, there is the appearance of a shoulder between 450–320 nm. This indicates the production of monohydroxy terephthalate groups and quinone species as described earlier.

3.1.4 | Summary

Results from the weatherometer exposures show the production of carboxylic acid end groups, dimers, anhydrides, monohydroxy terephthalate groups and quinone species. Mono-substituted rings have also been shown to

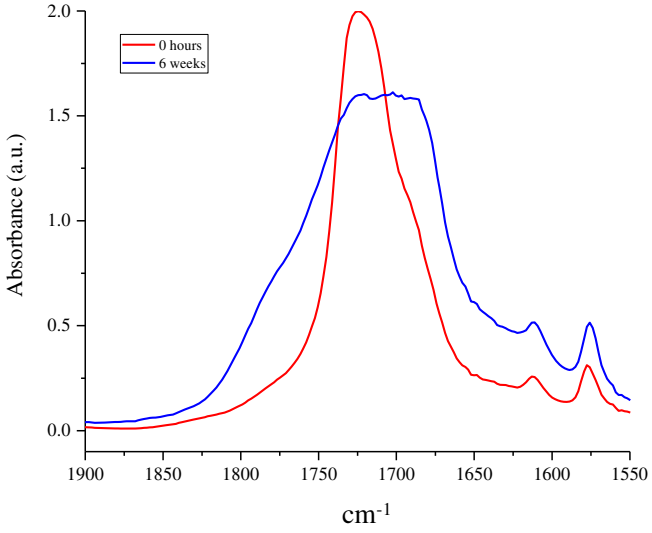

FIGURE 10 DRIFT spectra of PDEGT irradiated in the weatherometer, in the carbonyl region between 1850–1550 cm^{-1}. [Color figure can be viewed at wileyonlinelibrary.com]

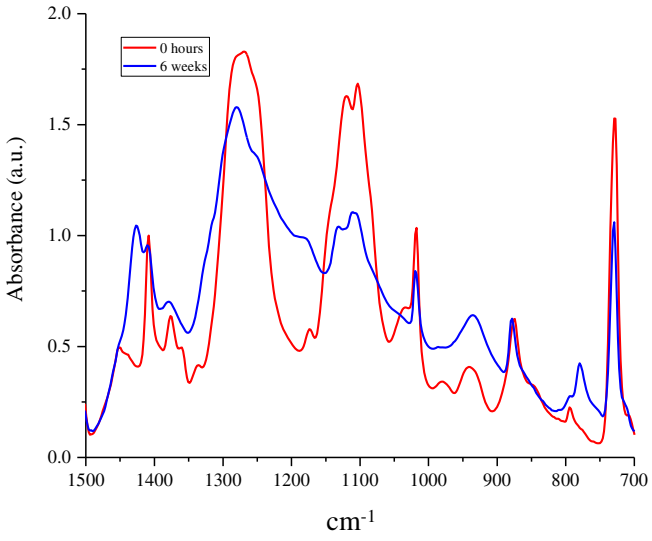

FIGURE 11 DRIFT spectra of PDEGT irradiated in the weatherometer, in the fingerprint region between 1500–700 cm^{-1}. [Color figure can be viewed at wileyonlinelibrary.com]

be produced by the development of a peak in both the ATR and DRIFT spectra.

PDEGT degrades to a greater extent than PET exposed under similar conditions, when irradiated in the weatherometer at the same temperature and time. This is thought to be due to the instability of the ether linkage although we do note that a factor may also be that difference that the exposures in the weatherometer were run at (37.5 ± 2.5)°C, which is above the T_g of PDEGT but below the T_g of PET.

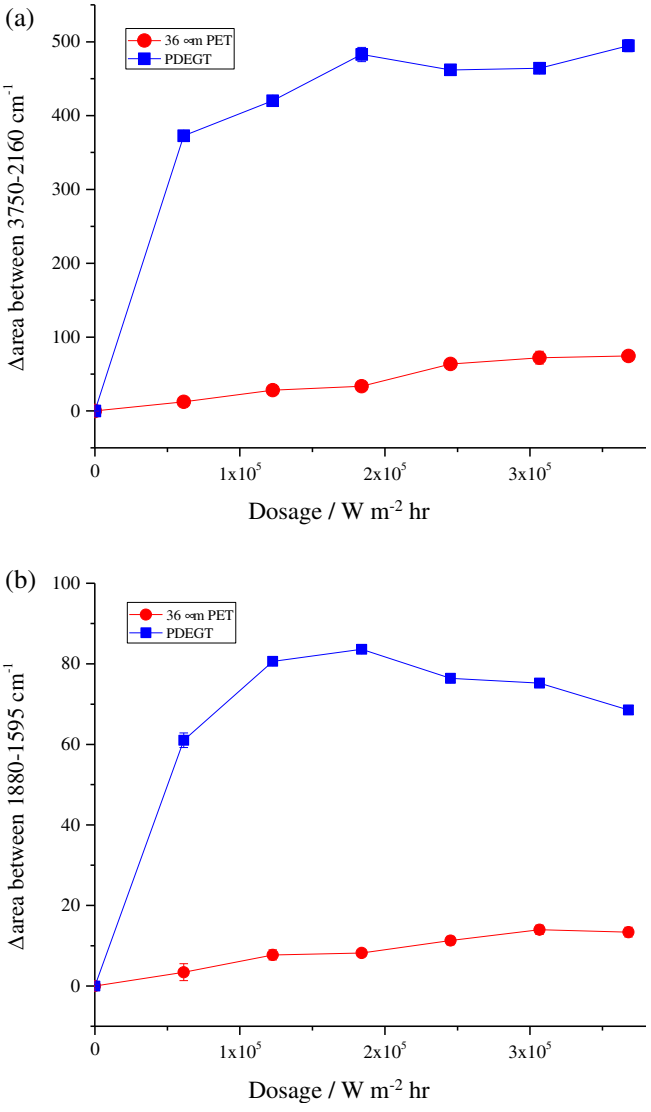

FIGURE 12 Extent of photodegradation of PDEGT measured by the change in area of DRIFT peaks between (a) 3750–2160 cm^{-1} and (b) 1880–1595 cm^{-1}. [Color figure can be viewed at wileyonlinelibrary.com]

3.2 | Effect of wavelength on the photodegradation of PDEGT

To better understand the data from weathering experiments under simulated sunlight, PDEGT was exposed to two specific wavelength ranges of UV - UV-A (365 nm) and UV-B (302 nm) - at room temperature for 168 hours (equivalent to a dosage of approximately 4.8 x 10^3 W m^{-2} h^{-1} and 4.2 x 10^3 W m^{-2} h^{-1}, respectively) in 24 h increments (equivalent to a dosage of approximately 8.3 x 10^2 W m^{-2} h and 6.1 x 10^2 W m^{-2} h, respectively). This allowed for the analysis of the effect of different wavelengths of light on the photodegradation of PDEGT. Samples were analyzed using ATR FT-IR, DRIFT and UV–Vis–NIR.

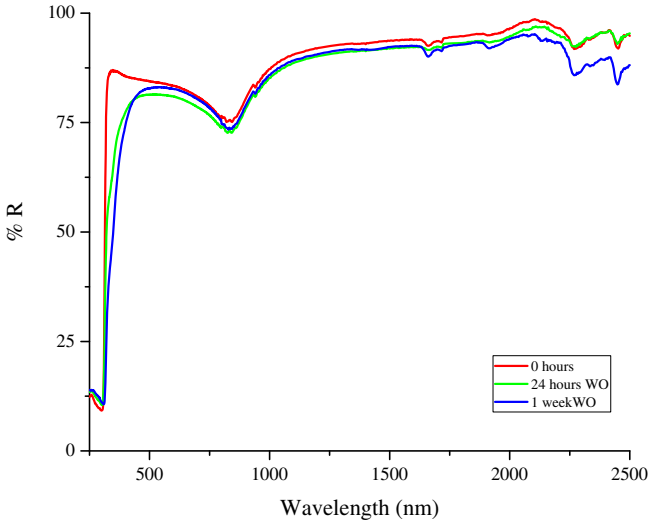

FIGURE 13 UV–Vis–NIR spectra of PDEGT samples irradiated in the weatherometer. [Color figure can be viewed at wileyonlinelibrary.com]

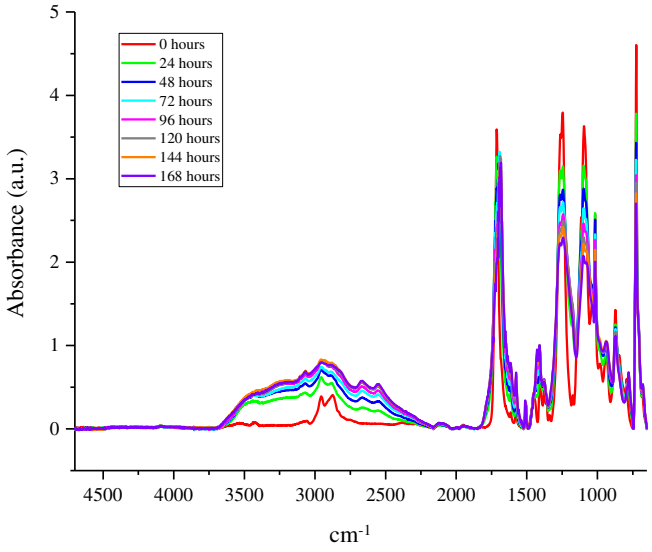

FIGURE 14 ATR FT-IR spectra of PDEGT exposed to 302 nm light for 1 week. [Color figure can be viewed at wileyonlinelibrary.com]

3.2.1 | ATR ft-IR

Figures 14 and 15 show the ATR spectra for the PDEGT samples exposed to 302 and 365 nm light, respectively.

Changes upon irradiation at 365 nm are minimal, but spectral changes upon completion of the exposure at 302 nm are very similar to those obtained upon weathering and comparison of the localized regions 3800–2100, 1850–1550 and 1500–700 cm^{-1} (supplementary material, Figures S5-S7) with the equivalent spectra from the completed weathering experiments (Figures 4 - 6) show

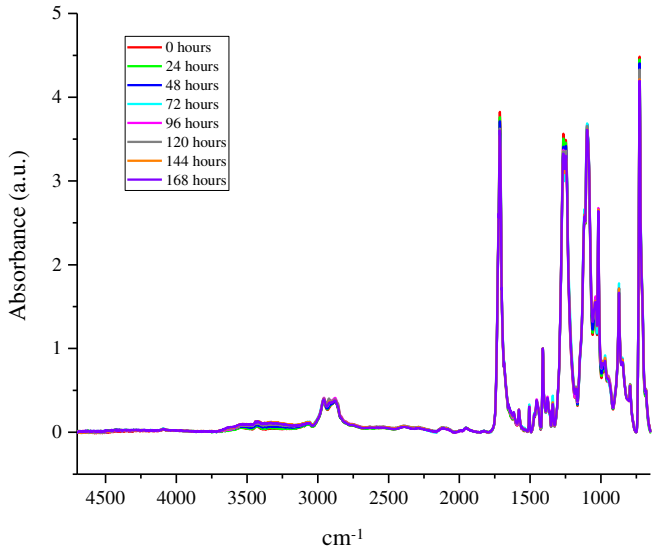

FIGURE 15 ATR FT-IR spectra of PDEGT exposed to 365 nm light for 1 week. [Color figure can be viewed at wileyonlinelibrary.com]

differences in subtle points of detail only, immediately suggesting that the bulk of the changes upon weathering are induced by wavelengths less than 365 nm.

The extent of photodegradation of PDEGT was measured by the change in area of the peaks in the region between 3800–2100 cm^{-1} and in the region 1880–1525 cm^{-1}. Figure 16a and b show the change in area of these peaks, with dosage, for PDEGT exposed to 302 nm and 365 nm light. For comparison data for 36 μm PET from reference 13 are included. Both (a) and (b) show that PDEGT exposed to 302 nm light degrades to a greater extent than PET in similar circumstance. Again, this suggests that the ether linkage is the weak link in PDEGT, as for thermal degradation, as this is the only structural difference between the two polymers. As with PET, PDEGT degradation is much less pronounced under 365 nm light. This was expected as PDEGT, like PET, shows a much stronger absorbance at shorter wavelengths (Figure 2). Indeed, samples of PDEGT and PET exposed to 365 nm light degrade to similar extents.

3.2.2 | Drift

The DRIFT spectra of PDEGT films exposed to 365 and 302 nm light for 1 week (equivalent to a dosage of approximately 4.8 x 10^3 W m^{-2} h and 4.2 x 10^3 W m^{-2} h, respectively) in 24 h increments (equivalent to a dosage of approximately 8.3 x 10^2 W m^{-2} h and 6.1 x 10^2 W m^{-2} h, respectively) are shown in Figures 17 and 18 and show similar trends to the ATR spectra. The

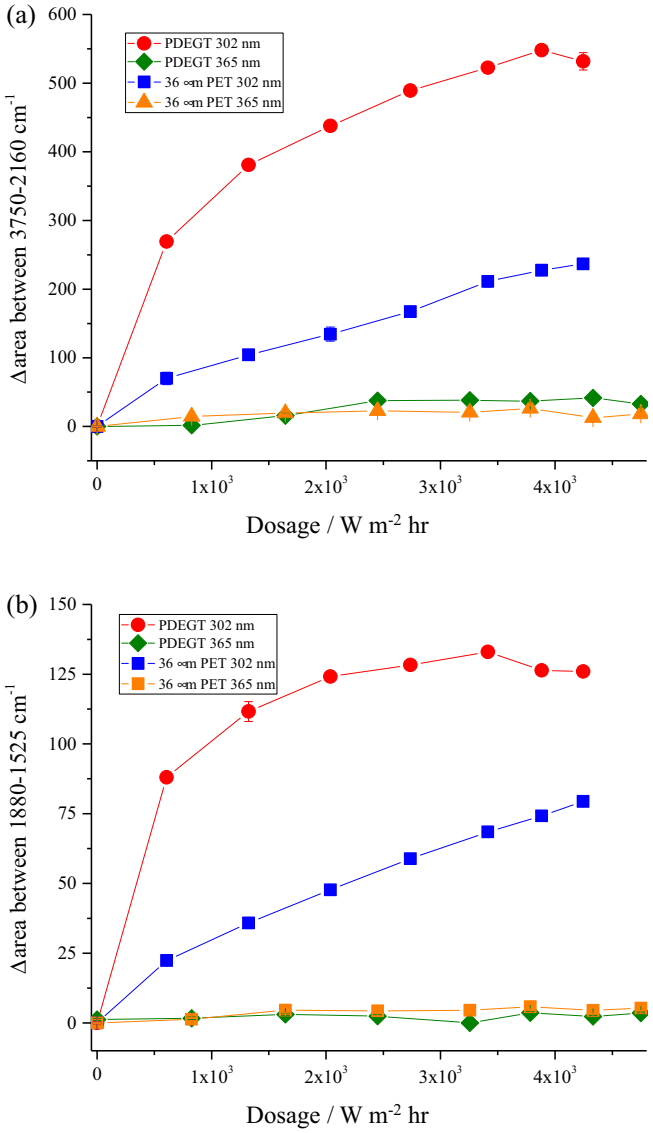

FIGURE 16 Extent of photodegradation of PDEGT measured by the change in area of peaks between (a) 3750–2160 cm^{-1} and (b) 1880–1525 cm^{-1}(carbonyl), from the ATR spectra. [Color figure can be viewed at wileyonlinelibrary.com]

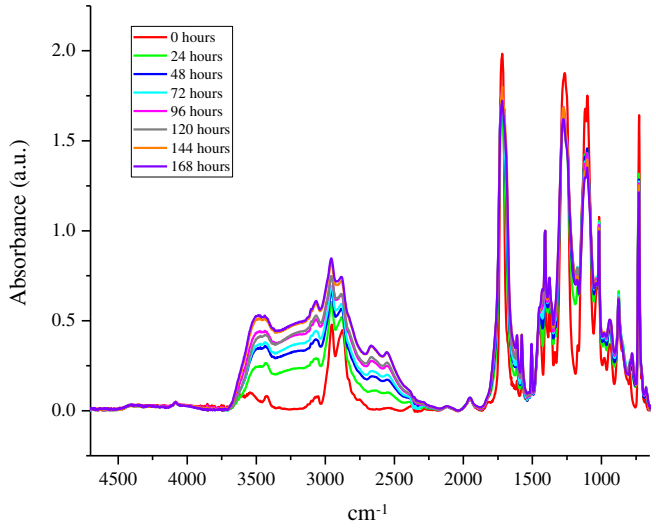

FIGURE 17 DRIFT spectra of PDEGT films exposed to 302 nm light for 1 week, in 24 h increments. [Color figure can be viewed at wileyonlinelibrary.com]

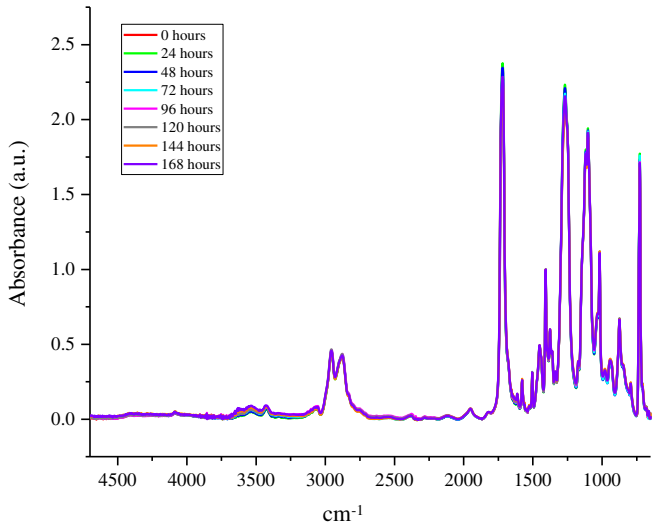

FIGURE 18 DRIFT spectra of PDEGT films exposed to 365 nm light for 1 week, in 24 h increments. [Color figure can be viewed at wileyonlinelibrary.com]

spectra of samples exposed to 302 nm light show that changes are apparent in the region between 3800–2100 cm^{-1}, as well as the carbonyl and fingerprint regions, after exposure. Again, however, samples exposed to 365 nm show only minor spectral changes.

3.2.3 | UV–Vis–NIR

UV–Vis–NIR was used to analyze PDEGT samples exposed to 302 nm and 365 nm light after 1 week. The spectra are shown in Figure 19. Table 4 gives the assignments for the peaks present in the spectra in Figure 19. Peaks at 2265 and 2450 nm have been assigned to a combination C-H stretching, while 1715, 1660 and 845 nm have been assigned to the first overtone and third overtone of the C-H stretching. After exposure to 302 nm light, there has been development of a small peak at 1925 nm, which is assigned to the combination O-H stretching vibration. This suggests that there has been production of new hydroxy groups, including carboxylic acid end groups, during exposure. The sample exposed to 302 nm light also shows the appearance of a shoulder between 450–320 nm, indicating the production of mono-hydroxy terephthalate groups (Scheme 2) and quinone

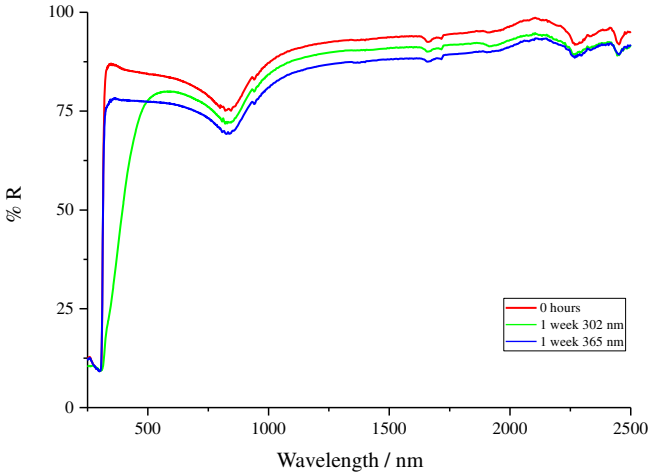

FIGURE 19 UV–Vis–NIR spectra of PDEGT samples exposed to 302 and 365 nm light. [Color figure can be viewed at wileyonlinelibrary.com]

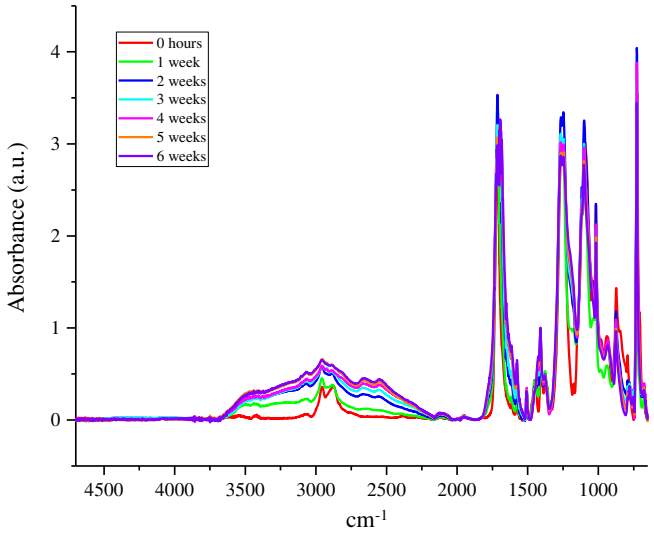

FIGURE 20 ATR FT-IR spectra of PDEGT exposed to 365 nm light for 6 weeks, in 1 week increments. [Color figure can be viewed at wileyonlinelibrary.com]

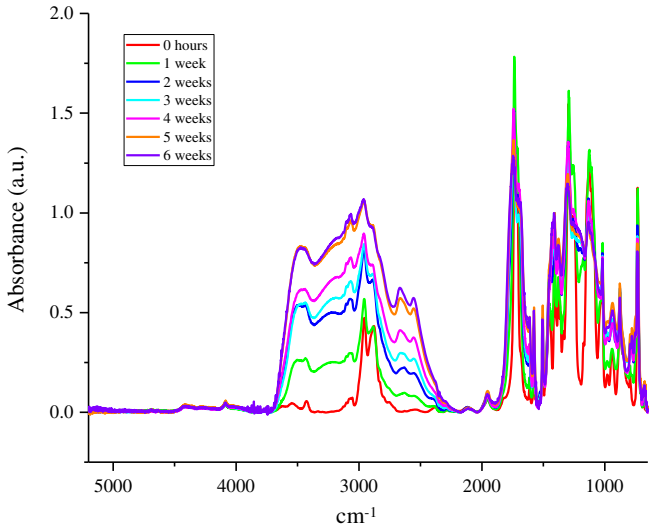

FIGURE 21 DRIFT spectra of PDEGT exposed to 365 nm light for 6 weeks, in 1 week increments. [Color figure can be viewed at wileyonlinelibrary.com]

species (Scheme 2) and is consistent with the observed slight yellowing of the film.

The spectrum for the PDEGT sample exposed to 365 nm light, depicted by the blue line in Figure 19, shows no meaningful change.

3.3 | Exposing PDEGT to high intensity 365 nm light

As minor changes were identified when PDEGT was exposed to 365 nm light at an average intensity of (31.7 ± 4.0) W m^{-2}, a more intense lamp, with an average intensity of (825.5 ± 20) W m^{-2}, was used to allow for any minimal changes to be highlighted. PDEGT films were exposed to high intensity 365 nm light at approximately (43 ± 2)°C for 6 weeks (equivalent to a dosage of approximately 8.3 x 10^5 W m^{-2} h^{-}) in 1-week increments, (equivalent to a dosage of approximately 1.4 x 10^5 W m^{-2} h^{-1}). Samples were analyzed, before and after exposure, using ATR FT-IR, DRIFT and UV–Vis–NIR.

3.3.1 | ATR FT-IR and DRIFT

The ATR FT-IR and DRIFT spectra of PDEGT exposed to high intensity 365 nm light, are shown in Figures 20 and 21, respectively. Peak assignments for the ATR and DRIFT spectra of PDEGT have already been discussed in detail. Both sets of spectra show significant change in the region between 3800–2100 cm^{-1} and in the carbonyl and fingerprint regions. The changes identified in both the ATR and DRIFT spectra follow the same trends as those seen in the weatherometer experiments.

Figure 20 shows that high intensity 365 nm light has had a significant effect on the surface of the PDEGT film. Clearly, at sufficiently high dosages, 365 nm light does induce degradation. Unlike 302 nm light, which is strongly absorbed and causes most degradation within only a few μm of the surface, 365 nm penetrates further with a significant degradative effect on the bulk of the film. Thus the DRIFT spectra, Figure 21, show more significant changes than the ATR spectra. PET has also been exposed to 365 nm light in a similar fashion[13] but does not show such a marked increase in the extent of degradation as seen with the PDEGT but does show greater

changes in the DRIFT spectra compared to the ATR spectra. It is important to note that the temperature of the irradiation chamber was (43 ± 2)°C, during exposures. This means that although PET was still below its T_g, PDEGT was exposed above its T_g and this may affect the rate of diffusion of oxygen and radical species in the bulk of the polymer.

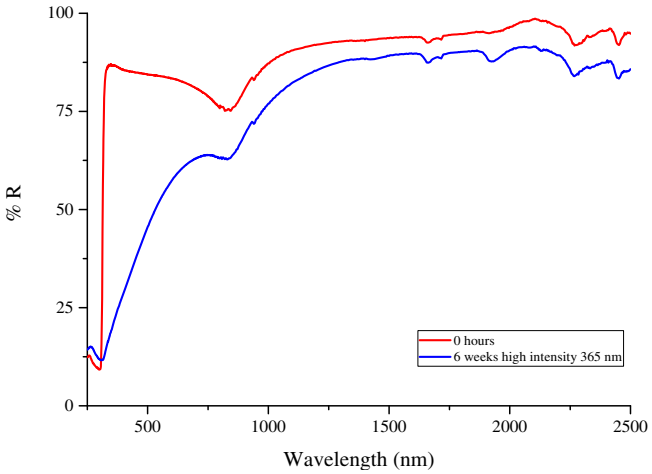

FIGURE 22 UV–Vis–NIR spectra of PDEGT before and after exposure to high intensity 365 nm light for 6 weeks. [Color figure can be viewed at wileyonlinelibrary.com]

3.3.2 | UV–Vis–NIR

Figure 22 shows the UV–Vis–NIR spectra for a control film and a PDEGT sample exposed to high intensity 365 nm light for 6 weeks. The peaks assignments for the UV–Vis–NIR spectra of PDEGT have been discussed in Section 3.2.3. The development of the peak at 1925 nm, assigned to the combination O-H stretching, indicates the production of new hydroxy groups, such as carboxylic acid end groups. After exposure, the spectra also show the appearance of a pronounced shoulder between 450–320 nm. This suggests the presence of monohydroxy terephthalate groups and quinone species, again reinforcing the conclusion that sufficiently high dosages of 365 nm UV will induce significant photodegradation.

3.3.3 | Summary

The effect of exposing PDEGT to different wavelengths of light was studied, using 302 and 365 nm light. PDEGT

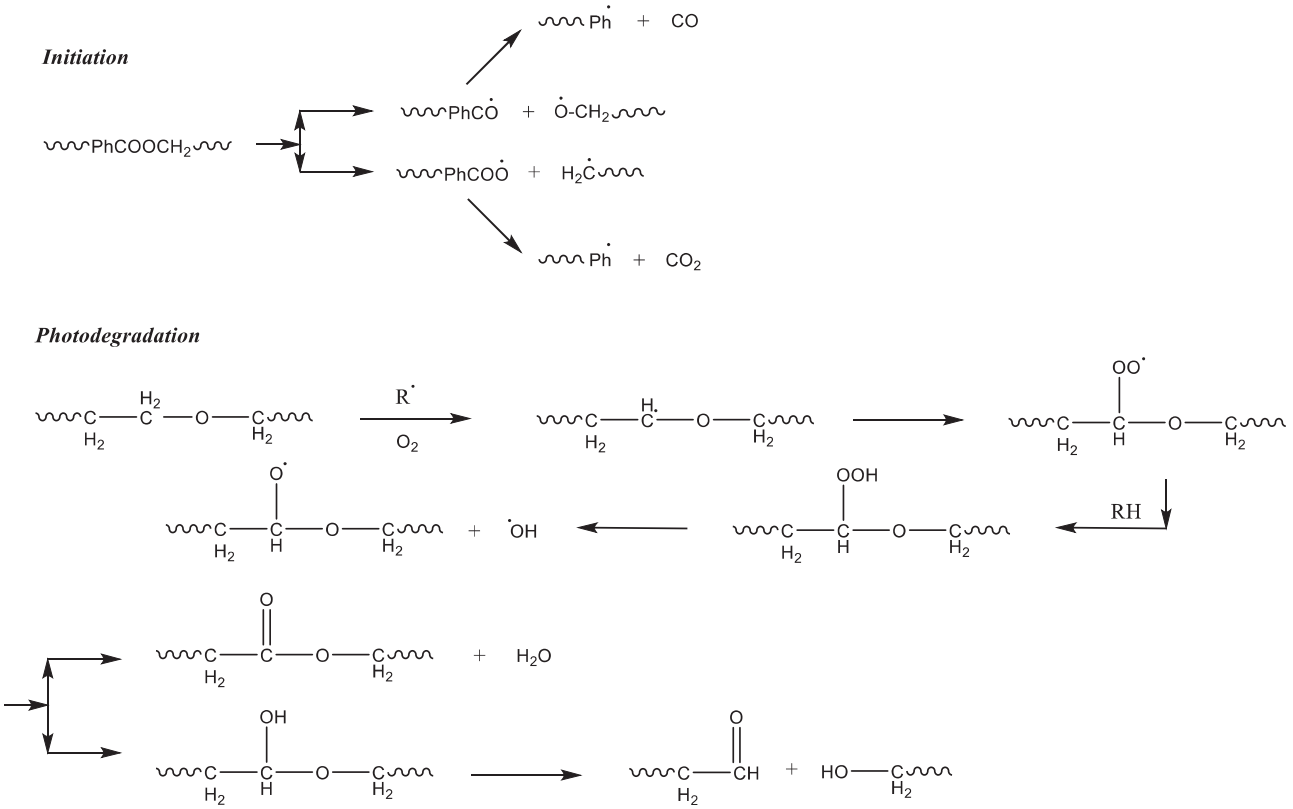

SCHEME 3 Mechanistic pathway for the photodegradation of PDEGT under oxidative conditions. Adapted for PDEGT from the model of Bei et al.[33]

samples exposed to 302 nm light showed production of carboxylic acid end groups, dimers, anhydrides, quinones, monohydroxy terephthalate groups and mono-substituted rings. The production of these groups suggests that chain scission and substitution reactions have occurred during exposure. Results show that PDEGT photodegrades faster under 302 nm light compared to 365 nm light of similar intensity, under oxidative conditions. This was expected as the UV–visible spectrum of PDEGT shows that longer wavelengths are absorbed weakly, whereas short wavelengths are absorbed strongly, with a λ_{max} of approximately 306 nm. Samples exposed to 365 nm light at similar dosages showed only minor changes with exposure time but higher dosages of 365 nm UV will induce significant photodegradation.

4 | CONCLUSIONS

Wang et al. reported that the photodegradation process of PET takes place in two steps; a very rapid initial step, due to the scission of weak links, followed by the degradation of normal links. The authors reported that the rate constants of degradation for weak links were higher than that for normal links, as the weak links are more easily broken.[32] The authors did not identify the weak links but it is very tempting on the basis of our data to associate them with DEG sequences introduced deliberately or adventitiously into the backbone. Certainly our data indicate that PDEGT degrades to a greater extent than PET when weathered under similar conditions although in a manner mechanistically very similar to that of PET. The fact that PDEGT degrades to a greater extent than PET is due to the susceptibility of the ether linkage.

Scheme 3 shows the proposed initiation free radical reactions as well as the mechanistic pathway for the photo-oxidation reactions occurring during the degradation of PDEGT. This mechanism is based on that proposed by Bei et al. for the photodegradation of polycaprolactone-poly(ethylene glycol) block copolymer.[33] These authors reported that pure poly(ethylene glycol) could not be photodegraded alone but increasing its content in the copolymer increased the rate of photodegradation. The authors concluded that this was due to the carbonyl groups in the poly(ε-caprolactone) segment "catalyzing" the scission of the poly(ethylene glycol) chains through secondary free radical reactions. The DEG sequences are not themselves photoactive over this wavelength range as the ether group absorption occurs below 200 nm and thus the DEG units are acting not as photochemical weak links, instead acting as additional sites for secondary free radical chemistry.

This is consistent with our work on the thermo-oxidative chemistry of PDEGT[12] where we noted that the higher sensitivity of α-ether CH_2 groups to radical formation, as reported by Botelho et al.,[10] plays an important role in the thermo-oxidative degradation of DEG units.

AUTHOR CONTRIBUTIONS

Fiona J. Horne: Conceptualization (equal); data curation (lead); formal analysis (lead); investigation (lead); methodology (equal); writing – original draft (lead). **John J. Liggat:** Conceptualization (equal); funding acquisition (lead); methodology (equal); project administration (lead); resources (lead); supervision (lead); writing – review and editing (lead).

ACKNOWLEDGMENTS

This work was supported by DuPont Teijin Films and the Strathclyde Centre for Doctoral Training in Advanced Functional and Engineering Polymers.

DATA AVAILABILITY STATEMENT

Data underpinning this publication are openly available from the University of Strathclyde Knowledge Base at https://doi.org/10.15129/653fed93-4fbb-4dbb-aa88-84ccc9640a65.

CONSENT FOR PUBLICATION

Consent for publication has been given by DuPont Teijin Films.

ORCID

John J. Liggat https://orcid.org/0000-0003-4460-5178

REFERENCES

[1] S. G. Hovenkamp, J. P. Munting, *J. Polym. Sci. Part A-1 Polym. Chem* **1970**, *8*, 679.
[2] L.-W. Chen, J.-W. Chen, *J. Appl. Polym. Sci.* **2000**, *75*, 1221.
[3] L.-W. Chen, J.-W. Chen, *J. Appl. Polym. Sci.* **2000**, *75*, 1229.
[4] H. Pohl, *J. Am. Chem. Soc.* **1951**, *73*, 5660.
[5] W. L. J. Hergenrother, *Polym. Sci. Polym. Chem. Ed.* **1995**, *12*, 875.
[6] L. H. Buxbaum, *Angew. Chem., Int. ed.* **1968**, *7*, 182.
[7] H. Zimmermann, in *Developments in Polymer Degradation*, Vol. 5 (Ed: N. Grassie), Applied Science Publishers, New York **1984**, p. 79.
[8] M. Bounekhel, I. C. McNeill, *Polym. Degr. Stab.* **1995**, *49*, 347.
[9] B. J. Holland, J. N. Hay, *Polymer* **2002**, *4*, 1835.
[10] G. Botelho, A. Queiros, P. Gijsman, *Polym. Degr. Stab.* **2000**, *67*, 13.
[11] W. A. MacDonald, *Polym. Int.* **2002**, *51*, 923.
[12] H. A. Lecomte, J. J. Liggat, *Polym. Degr. Stab.* **2006**, *91*, 681.
[13] F. J. Horne, J. J. Liggat, W. A. MacDonald, S. W. Sankey, *J. Appl. Polym. Sci.* **2020**, *137*, 48623.
[14] D. Burnett, E. Barbour, G. Harrison, *Renewable Energy* **2014**, *71*, 333.

[15] M. Day, D. M. Wiles, *J. Appl. Polym. Sci.* **1972**, *16*, 175.
[16] C. F. L. Ciolacu, N. Roy Choudhury, N. K. Dutta, *Degrad. Stab.* **2006**, *91*, 875.
[17] A. K. Crane, E. Y. L. Wong, M. J. MacLachlan, *Cryst. Eng. Comm.* **2013**, *15*, 9811.
[18] P. Delprat, X. Duteurtreb, *Polym. Degrad. Stab.* **1995**, *50*, 1.
[19] M. Day, D. M. Wiles, *J. Appl. Polym. Sci.* **1972**, *16*, 191.
[20] N. S. Allen, M. Edge, M. Mohammadian, K. Jones, *Polym. Degrad. Stab.* **1994**, *43*, 229.
[21] G. J. M. Fechine, M. S. Rabello, R. M. Souto Maior, L. Catalani, *H. Polymer* **2004**, *45*, 2303.
[22] Z. Chen, J. N. Hay, M. J. Jenkins, *Eur. Polym. J.* **2012**, *48*, 1586.
[23] N. B. Colthup, L. H. Daly, S. E. Wiberley, *Introduction to Infrared and Raman Spectroscopy*, 3rd ed., Academic Press, London **2009**.
[24] C. V. Stephenson, C. Lacey, W. S. Wilcox, *J. Polym. Sci.* **1961**, *55*, 477.
[25] J. Scheirs, J. L. Gardette, *Polym. Degrad. Stab.* **1997**, *56*, 339.
[26] A. Rivaton, J. L. Gardette, C. E. Hoyle, M. Ziemer, D. R. Fagerburg, H. Clauberg, *Polymer* **2000**, *41*, 3541.
[27] J. V. Gulmine, P. R. Janissek, H. M. Heise, L. Akcelrud, *Polym. Degrad. Stab.* **2003**, *79*, 385.
[28] M. Edge, R. Wiles, N. S. Allen, W. A. MacDonald, S. V. Mortlock, *Polym. Degrad. Stab.* **1996**, *53*, 141.
[29] G. J. M. Fechine, M. S. Rabello, R. M. Souto Maior, *Polym. Degrad. Stab.* **2002**, *75*, 153.
[30] J. G. Pacifici, J. M. Straley, *Polym. Lett.* **1969**, *7*, 7.
[31] M. Day, D. M. Wiles, *J. Appl. Polym. Sci.* **1972**, *16*, 203.
[32] W. E. I. Wang, A. Taniguchi, M. Fukuhara, T. Okada, *J. Appl. Polym. Sci.* **1998**, *74*, 306.
[33] J. Bei, W. He, X. Hu, S. Wang, *Polym. Degrad. Stab.* **2000**, *67*, 375.

SUPPORTING INFORMATION

Additional supporting information can be found online in the Supporting Information section at the end of this article.

How to cite this article: F. J. Horne, J. J. Liggat, *J. Appl. Polym. Sci.* **2023**, e53760. https://doi.org/10.1002/app.53760